

Rodolfo Montironi · Adhemar Longatto Filho  
Alfredo Santinelli · Roberta Mazzucchelli  
Roberto Pomante · Paola Colanzi · Marina Scarpelli

# Nuclear changes in the normal-looking columnar epithelium adjacent to and distant from prostatic intraepithelial neoplasia and prostate cancer

## Morphometric analysis in whole-mount sections

Received: 26 May 2000 / Accepted: 6 July 2000 / Published online: 18 October 2000  
© Springer-Verlag 2000

**Abstract** Subtle morphological changes and molecular alterations have been reported in normal-appearing tissue in prostates with high-grade prostatic intraepithelial neoplasia (PIN) and prostate cancer (PCa). The severity and the distribution of these changes and alterations within the prostate gland have not been addressed in previous publications. The aim of this study was to investigate morphometrically the nuclear changes of the normal-looking columnar epithelium adjacent to and distant from high-grade PIN and PCa. Karyometry was performed on the whole-mount histological sections of three radical prostatectomy (RP) specimens. Two concentric lines, one corresponding to the outer surface (or capsule) of the prostate and the other corresponding to one centimeter towards the center, were drawn with a black pen on each whole-mount section. The part of the prostate tissue between these two boundaries was then divided into twelve equal sectors or regions. The part within the inner line was divided into two regions. The analysis was also performed on the slides of the apex and base of the prostate. One prostate contained normal-looking epithelium only (case no. 1). Another contained both high-grade PIN and PCa, the former occupying larger areas than the latter (case no. 2). Both high-grade PIN and PCa were present in the third sample, in which PCa was more widely distributed than PIN (case no. 3). The lesion measured in each region was always the most severe, e.g., either high-grade PIN or PCa. When neither were identifiable, then the normal-looking columnar epithelium was analyzed. For each sector, the mean and standard deviation of the nuclear area, maximum nuclear diameter, nuclear roundness factor, and nucleolar area

were calculated. In normal-looking columnar epithelium, the mean of the mean nuclear area of the sectors of case no. 1 was  $35.19 \mu\text{m}^2$  (SD 4.14). The mean nuclear areas in cases no. 2 and no. 3 were  $37.94 \mu\text{m}^2$  (SD 4.65) and  $37.31 \mu\text{m}^2$  (SD 4.36), respectively. The mean of the mean nuclear area of the sectors with high-grade PIN of case no. 2 was  $49.85 \mu\text{m}^2$  (SD 8.44), whereas it was  $54.26 \mu\text{m}^2$  (SD 2.91) in case no. 3. The mean of the nuclear area values obtained in the sectors of cases no. 2 and no. 3 with PCa was  $56.74 \mu\text{m}^2$  (SD 6.56) and  $61.17 \mu\text{m}^2$  (SD 8.13), respectively. When considering the normal-looking tissue of the second and third case, 79% and 90%, respectively, of the regions showed nuclear area values greater than  $34.94 \mu\text{m}^2$  (e.g., the 50th percentile of the mean nuclear area values of the regions of the first case). Sectors with normal-looking epithelium, whose nuclear area was above this threshold, were both adjacent to and at a distance of more than 1 cm from those with PIN or PCa. The other nuclear features showed a similar trend of value changes. This study demonstrates that the normal-looking ducts and acini from prostate harboring preneoplastic and neoplastic lesions show morphological nuclear abnormalities that are not seen by the human eyes but that can be detected with image analysis. Such changes may be of diagnostic importance, especially in cases where clinical suspicion for cancer prevails after a negative biopsy.

**Keywords** Prostate · Normal prostate · Prostatic intraepithelial neoplasia · PIN · Prostate cancer · malignancy-associated changes · Karyometry · Quantitative analysis · Morphometry

R. Montironi (✉) · A.L. Filho · A. Santinelli · R. Mazzucchelli  
R. Pomante · P. Colanzi · M. Scarpelli  
Institute of Pathological Anatomy and Histopathology,  
School of Medicine, University of Ancona,  
Ospedale Regionale, I-60020 Torrette, Ancona, Italy  
e-mail: r.montironi@popcsi.unian.it  
Fax: +39-071-889985

## Introduction

High-grade prostatic intraepithelial neoplasia (PIN) is considered the precursor of prostate cancer (PCa) of the peripheral zone [1, 10, 21, 25, 29, 30, 31]. These studies

have shown that there are close similarities from the morphological, immuno-histochemical, and molecular points of view between high-grade PIN and PCa. The investigations, when made in whole-mount sections, have allowed the accurate identification of spatial and zonal distribution of these lesions. In particular, it has been demonstrated that high-grade PIN usually arises in the peripheral zone of the prostate, the area in which the majority (i.e., 70%) of prostatic cancers occur, and both lesions are frequently multifocal, indicating a "field" effect [14, 15, 20, 26, 28].

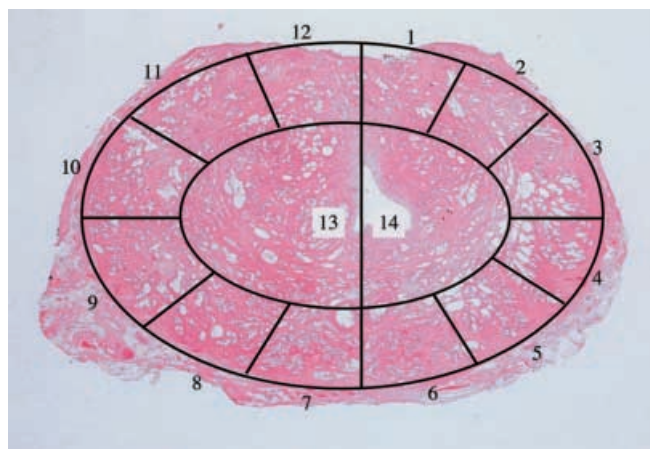
Subtle morphological changes, called malignancy-associated cellular markers or malignancy-associated changes, have been reported in normal-appearing tissue in prostates with high-grade PIN and PCa [3, 19, 24]. Two recent papers have addressed this issue by using image analysis techniques and have demonstrated that the normal-looking epithelium shows sub-visual abnormalities in the distribution of the nuclear chromatin [3, 19]. In one of these two studies, the non-malignant tissue surrounding the PCa was compared with tissue from the transition zone affected by benign prostatic hyperplasia (BPH) [19]. In the other study, abnormalities were detected up to 6 mm away from PIN and PCa. The analysis was conducted in the peripheral zone and using only a glass slide of a conventional size (e.g., 76×26 mm) per case [3]. At present, information is not available on how diffuse the epithelial abnormalities of the normal-looking ducts and acini can be in radical prostatectomy (RP) specimens with PCa and PIN.

The aim of this study was to investigate karyometrically the severity and the spatial distribution of the nuclear changes of normal-looking columnar epithelium in whole-mount sections of RP specimens containing both high-grade PIN and PCa.

## Materials and methods

Three RP specimens, examined with the whole-mount technique, were used in this study. The criterion adopted in the selection of this material was to have a prostate without morphologically detectable preneoplastic and neoplastic lesions [case no. 1: 55 years old; prostate volume (specimen measured with the ellipsoid volume formula) 44.75 cc], a prostate in which a limited amount of cancer was present, high-grade PIN, and normal-looking tissue being identifiable in several areas (case no. 2: 60 years old; prostate volume 39.55 cc), and a prostate in which cancer occupied a great proportion of the gland, high-grade PIN, and normal-looking prostate being also recognizable (case no. 3: 65 years old; prostate volume 36.63 cc). The first prostate was removed together with the bladder because of bladder cancer. Bladder cancer did not involve the prostate. The second and the third were removed because of PCa. Inflammation, BPH, or low-grade PIN was not identified in any of the three cases. None of the patients had received chemo-, hormone- or radiation therapy before surgery.

The material had been processed at the Institute of Pathological Anatomy and Histopathology of the University of Ancona School of Medicine. Briefly, the RP specimens had been covered with India ink and fixed for 24 h in neutral buffered formalin (4%). To enhance a quick and uniform penetration of the fixative, prostate specimens were injected with formalin solution. The rationale behind the injection procedure was that, during immersion in a formalin solution, the fixative only slowly diffuses toward the














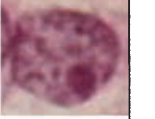
**Fig. 1** Whole-mount section from case no. 1. This section is close to the prostate base (e.g., F). The black lines divide the tissue into 14 sectors, 12 roughly corresponding to the non-transition zone (e.g., peripheral and central zones according to McNeal) and two to the transition zone

center of the specimens. When the periphery of the prostate is fixed, the presence of cross-linked proteins is thought to hinder further diffusion of the fixative toward the center of the specimen (so-called crust effect). After fixation, the prostate specimens had been step-sectioned at 0.5-cm intervals perpendicular to the long axis (apical to basal) of the gland. The distal (apical) and proximal (basal) parts of the prostates and the seminal vesicles had been removed from the RP specimens and submitted for histologic examination. The cut specimens had been post-fixed for an additional 24 h and then dehydrated in a graded alcohol series, cleared in xylene, embedded in paraffin, and examined histologically as 5-μm thick whole-mount sections. The number of sections differed between the three prostates, depending on the size of the RP specimen. The size of the glass slide used for this study was 76×50 mm. The whole-mount sections were identified in a consecutive manner with capital letters (A, B, etc), always starting from the most apical section.

## Quantitative analysis

Quantitative analysis was performed by one of us (ALF) on hematoxylin and eosin-stained histological sections. For the purpose of the analysis, two concentric lines, one corresponding to the outer surface (or capsule) of the prostate and the other 1 cm towards the center, were drawn with a black pen on each whole-mount section. The part of the prostate between these two boundaries, roughly corresponding to the non-transition zone (e.g., peripheral and central zones according to McNeal), was then divided into twelve equal sectors numbered clockwise from 1 to 12. The length of each sector along its external contour was at least 1 cm. The part of the prostate delimited by the inner line was divided into two halves or regions (e.g., sectors 13 and 14), as shown in Fig. 1. The quantitative evaluation was also performed on the histological sections of the apex and base (each slide was considered as a region or sector).

The lesion measured in each sector was always the most severe, e.g., either high-grade PIN or PCa. When neither lesions were identifiable, then the normal-looking columnar (secretory) epithelium was analyzed. A Zeiss-Kontron IBAS-AT Image Analyzer (Munich, Germany) combined with a Zeiss light microscope equipped with a 100× oil immersion objective was used. All distinguishable nuclei in a microscopic measurement field were systematically selected, starting from the upper left corner of the measurement field. To find the number of nuclei to be measured, the running mean procedure was applied. The measurement of 30

Normal-looking epithelium								
	•Case No	1	2	2	3			
	•NA	31.19	33.22	37.34	40.58			
	•ND	6.91	7.21	7.81	8.01			
	•NRF	0.97	0.92	0.95	0.98			
	•NuA	1.23	1.41	1.75	1.51			
High-grade PIN								
	•Case No	2	2	3	3			
	•NA	48.22	53.19	51.49	58.37			
	•ND	8.91	9.37	9.41	8.88			
	•NRF	0.94	0.95	0.95	0.98			
	•NuA	2.35	2.79	2.49	2.72			
Prostatic carcinoma								
	•Case No	2	2	3	3			
	•NA	55.33	52.41	60.33	65.21			
	•ND	9.22	9.75	8.95	10.22			
	•NRF	0.93	0.96	0.98	0.95			
	•NuA	3.39	3.59	2.92	3.21			

**Fig. 2** Gallery of individual nuclei with their corresponding feature values. The first row shows nuclei that look morphologically very alike; however, differences are detected karyometrically. Nuclei from the prostatic intraepithelial neoplasia (PIN) and prostate cancer (PCa) sectors are shown for comparison in the *second* and *third* rows

nuclei was sufficient to have a cumulative average within the 95% limits. To be sure of adequate sampling, 50 nuclei were measured in each case. The selected nuclei had clearly visible boundaries. Disintegrated nuclei or disintegrated cells were not measured.

The resulting measurements were recorded and, for each sector, the mean and standard deviation of the following features were calculated (nuclear area, maximum nuclear diameter, nuclear roundness factor, and nucleolar area). The maximum nuclear diameter is the largest of the Feret diameters, measured in 32 different directions (i.e., at an angular resolution of 5.7°). The nuclear roundness factor is a size-independent indicator of the regularity of a profile. It was calculated according to the following formula: 1 divided by  $(4 \times \pi \times \text{nuclear area} \div \text{squared nuclear perimeter})$ . Its value is 1.0 for a circle and below 1.0 for irregular structures. When a nucleus contained more than one nucleolus, all the nucleoli were evaluated, and their area was summed up. Therefore, in our study, the nucleolar area was derived from the total nucleolar area of each nucleus.

The intra- and inter-observer variation was assessed in six sectors, two for each case. Two observers (RP and AS) performed the measurements. Correlation coefficients greater than 0.95 were obtained in the repeated measurements of the nuclear area, maximum nuclear diameter, and nucleolar area. The nuclear roundness factor was less reproducible, the correlation coefficients of the repeated evaluations being lower than 0.90.

The Z-score transformation of the mean sector value of each feature was also performed in order to have all of the features expressed in the same scale of values. To do this, the mean and standard deviation of the normal-looking tissue of case no. 1 were used to transform the feature values of all of the sectors of all of

the cases. The following formula was used:  $Z_i = (X_i - M) / SD$ , where  $Z_i$  is the Z-score of a given sector,  $X_i$  is the mean value of the same sector, and  $M$  and  $SD$  are the mean and SD of the feature mean values of the sectors of case no. 1. As an example, when considering the nuclear area (expressed in square micrometers), the mean and SD of case no. 1 are 35.19 and 4.14, the mean value of sector no. 6 of the most apical whole-mount section being 32.75. Then, the Z-score of this sector is  $(32.75 - 35.19) / 4.14 = -0.589$ .

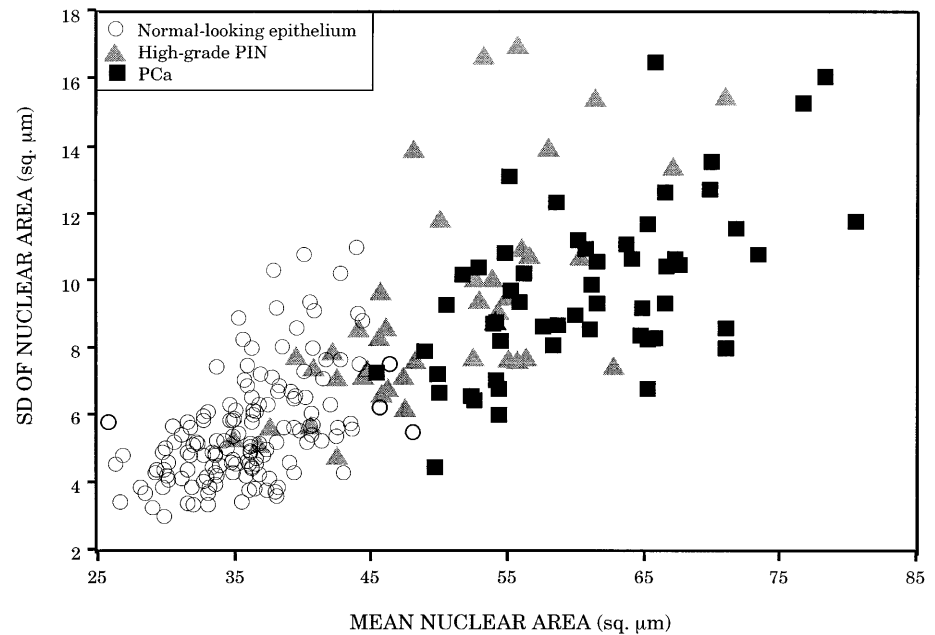
Statistical analysis was done using a Macintosh computer with StatView (Abacus Concepts, Inc., Berkeley, Calif.). Nonparametric tests, e.g., Mann-Whitney, Kruskal-Wallis, and Spearman's rank correlation tests, were used.

## Results

Ninety-nine sectors were identified in case no. 1, 80 in case no. 2, and 65 in case no. 3. Normal-looking tissue was present in 100, 47, and 15% of the sectors of cases no. 1, no. 2, and no. 3, respectively. High-grade PIN was identified in 47% and 6% of the sectors of cases no. 2 and no. 3, PCa being present in 6% and 79% of the sectors, respectively. The Gleason sum of the PCa of the second and third prostate was 6 and 7, respectively. Both were of stage pT2b N0 M0 R0.

Figure 2 shows a gallery of nuclei of normal-looking tissue, high-grade PIN, and PCa. The nuclei from normal-looking tissue looked morphologically similar. However, they differ from the morphometrical point of view. Nuclei from PIN and PCa are shown for comparison. These nuclei appeared different both histologically and morphometrically from those of the normal-looking tissue.

**Fig. 3** A scattergram obtained with the mean and SD of the nuclear area of each sector. There is a continuum from normal-looking epithelium to prostatic intraepithelial neoplasia (PIN) and prostate cancer (PCa). A certain degree of overlap exists between the values of normal-looking epithelium and those of PIN



Concerning normal-looking columnar epithelium, the mean nuclear area of all sectors of case no. 1 was  $35.19 \mu\text{m}^2$  (SD 4.14). The mean of the same features in cases no. 2 and no. 3 was  $37.94 \mu\text{m}^2$  (SD 4.65) and  $37.31 \mu\text{m}^2$  (SD 4.36), respectively. The differences were statistically significant (Kruskal-Wallis test;  $P=0.0005$ ). The mean of the mean nuclear area of the sectors with high-grade PIN of case no. 2 was  $49.85 \mu\text{m}^2$  (SD 8.44), whereas it was  $54.26 \mu\text{m}^2$  (SD 2.91) in case no. 3. The differences were not statistically significant (Mann-Whitney test;  $P=0.1574$ ). The mean of the nuclear area values obtained in the sectors of cases no. 2 and no. 3 with PCa was  $56.74 \mu\text{m}^2$  (SD 6.56) and  $61.17 \mu\text{m}^2$  (SD 8.13), respectively. The differences were not statistically significant (Mann-Whitney test;  $P=0.2566$ ).

The other nuclear features showed a similar trend of value changes (data not shown). The values of the nuclear area were highly correlated with those of the maximum nuclear diameter (correlation coefficient: 0.99). Correlation coefficients lower than 0.90 were seen between these two features and nuclear roundness factor and nucleolar area.

Figure 3 shows the scattergram obtained with the following two features: mean and SD of the nuclear area of each sector. There is a continuum from normal-looking epithelium to PIN and PCa, which extends from the lower left corner of the bivariate graph to the upper right corner. A quite extensive overlap exists between the values of PIN and those of PCa. When considering normal-looking epithelium, there are two groups of sectors, one separated from PIN and located in the lower left corner of the bivariate graph and the other showing overlap with those of PIN.

Figure 4, Fig. 5, and Fig. 6 report graphically the value of the mean nuclear area for each sector of the whole-mount sections of the three cases. The horizontal line in

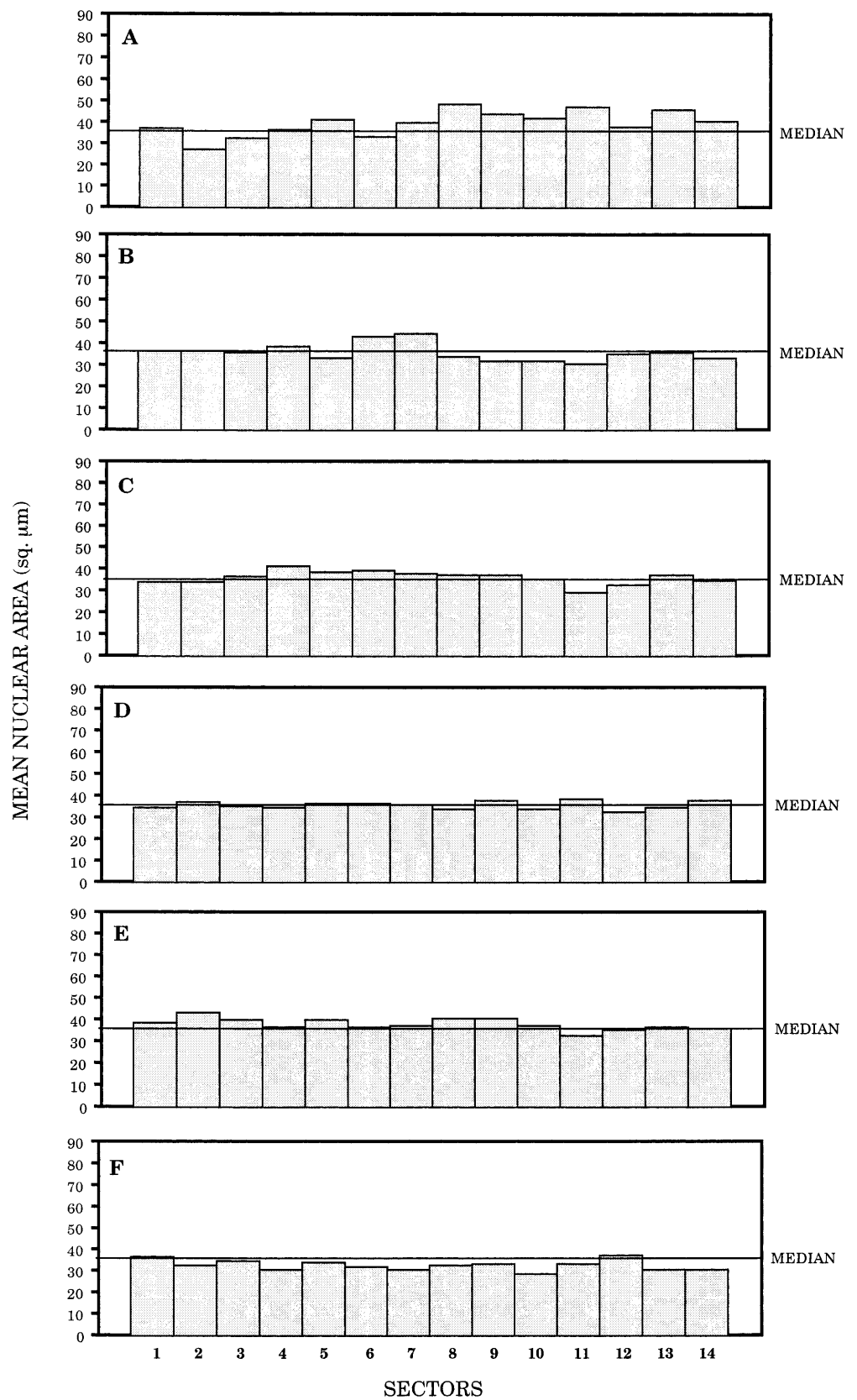
each graph is the 50th percentile or median of the mean nuclear area of the sectors of case no. 1 (e.g.,  $34.94 \mu\text{m}^2$ ). Concerning normal-looking epithelium, 50% of the regions of case no. 1 are above it, whereas in case no. 2 and case no. 3, the proportions are 79% and 90%, respectively. All PIN and PCa regions are above it. When the threshold is set at the 75th percentile of the mean nuclear area of normal-looking epithelium of case no. 1 (e.g.,  $37.33 \mu\text{m}^2$ ), the proportions of regions whose nuclear area values are greater than this threshold are 25%, 58%, and 60%, respectively in cases no. 1, no. 2, and no. 3. The sectors with high-grade PIN and PCa are all above this percentile. In case no. 1, most of the sectors with nuclear area values above this percentile were clustered in the prostate sections taken from the most apical part of the gland.

Figure 5 and Fig. 6 also show that the regions of normal looking epithelium with nuclear area greater than  $34.94 \mu\text{m}^2$  are both adjacent to the sectors with PIN and PCa and distant from them (the nuclear area values of the normal-looking epithelium adjacent to PIN and those adjacent to PCa did not show statistically significant differences). Since the length of an individual sector along its external contour is equal to 1 cm or even greater than this, these figures show that, within an individual whole-mount section, the normal-looking epithelium with a nuclear area above the 50th percentile are present at a distance of more than 1 cm from the lesion. Such sectors belong both to the non-transition and transition zones of the gland. Since the whole-mount sections were cut from adjacent slices of prostate of 0.5 cm in thickness, Fig. 5 and Fig. 6 show how the nuclear area of the normal-looking epithelium changes from section to section in an apical to basal direction.

The other nuclear features showed a trend of value changes similar to those of nuclear area. As an example,



**Fig. 4** Mean nuclear area for each sector of the whole-mount sections of case no. 1. The *horizontal line* in each graph is the 50th percentile or median of the mean nuclear area. Of the sectors, 50% have a nuclear area above it. Each *column* represents a sector. Sector no. 1 is the *first column* on the *left* of the graph



**Fig. 5** Mean nuclear area for each sector of the whole-mount sections of case no. 2. The sectors of normal-looking epithelium are in *light gray color*, while those of prostatic intra-epithelial neoplasia (PIN) and prostate cancer (PCa) are in *dark gray and black colors*, respectively (the same applies to Fig. 6 and Fig. 7). All PIN and PCa regions are above the 50th percentile of the mean nuclear area of the sectors of the case no. 1 (*horizontal line in each graph*). Concerning normal-looking epithelium, 79% of the regions, including those of the apex and base, are above it

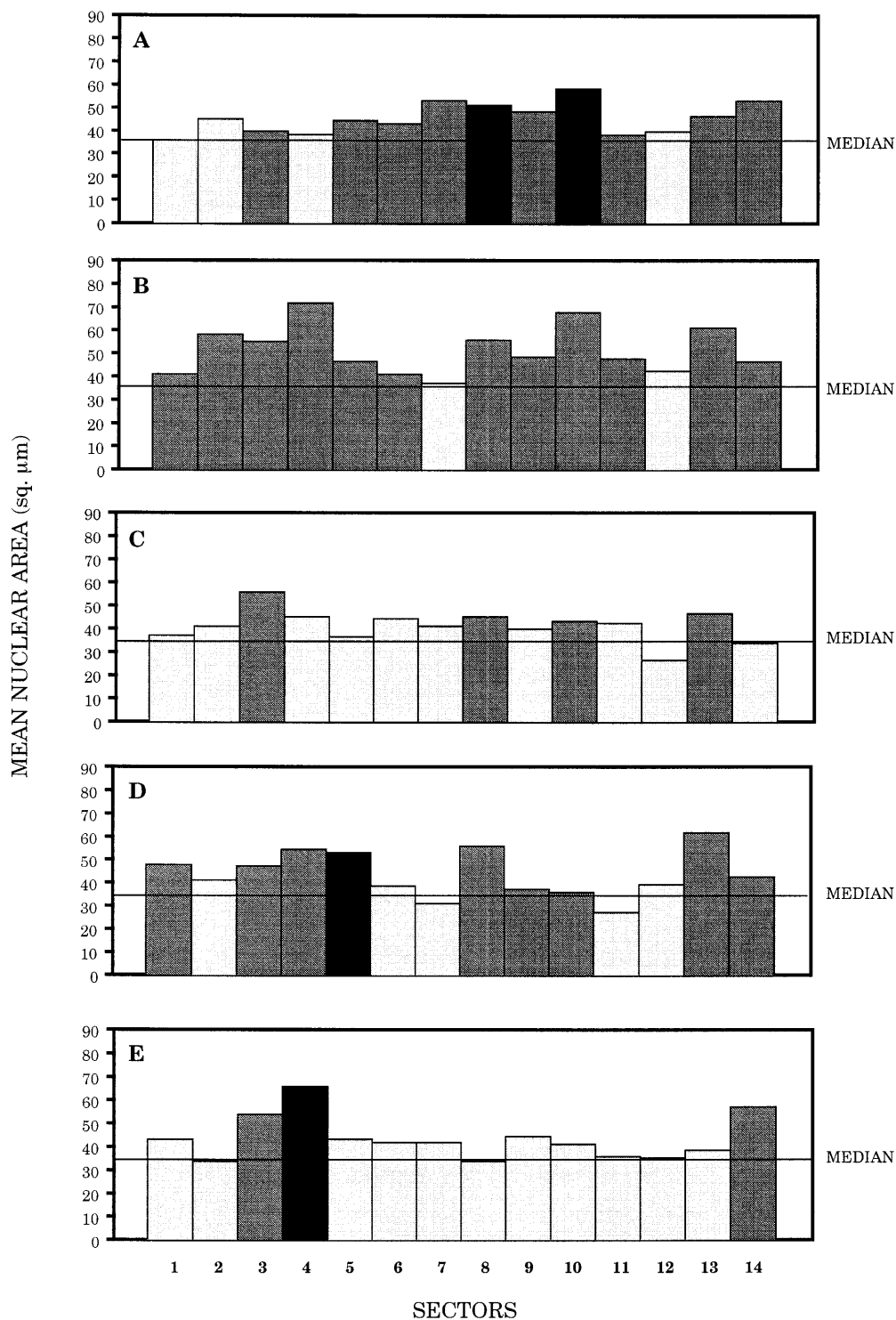
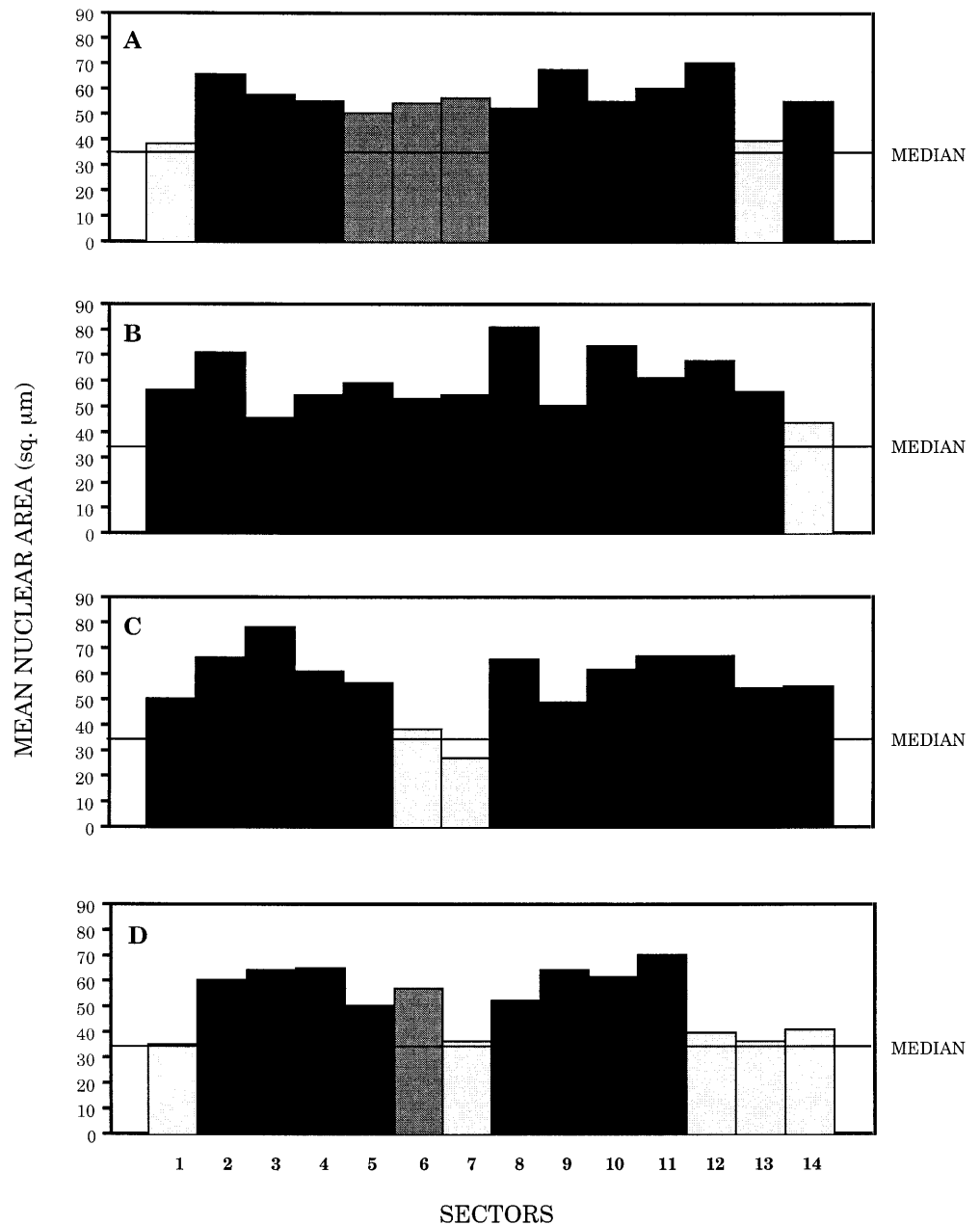


Fig. 7 shows graphically the values (expressed in Z-scores) of all of the nuclear features of sector no. 6, which is located in the posterior part of the non-transition zone of the prostate, for all of the whole-mount sections. In case no. 1, the profile of the sector feature values differs only slightly from one whole-mount section to another, the difference being sharp in the comparison

with the sectors with PIN or PCa. The sectors of normal-looking tissue of cases no. 2 and no. 3 show a pattern of feature value profile which is intermediate between that seen in case no. 1 and that associated with PIN or PCa.

**Fig. 6** Mean nuclear area for each sector of the whole-mount sections of case no. 3. All prostatic intraepithelial neoplasia (PIN) and prostate cancer (PCa) regions are above the 50th percentile of the mean nuclear area of the sectors of case no. 1 (*horizontal line in each graph*). Concerning normal-looking epithelium, 90% of the regions, including those of the apex and base, are above it



## Discussion

The present image analysis-based investigation demonstrates that the nuclei of the normal-looking epithelium of the two prostates with PIN and PCa show a diffuse abnormality which is intermediate in severity between that seen in case no. 1, where only normal-appearing tissue was present, and that of PIN and PCa.

The normal-looking tissue in prostates with PIN and PCa was investigated quantitatively in two previous studies [3, 19]. Bartels et al. [3] documented changes in the chromatin pattern in secretory cell nuclei. High-resolution images of nuclei were recorded, and a set of features descriptive of the chromatin texture and spatial distribution were computed. From these data-sets, features undergoing

a monotonic trend of progression were selected and plotted to reveal trends of progression from PIN to PCa [2]. Sets of images were also recorded in the histologically normal-appearing tissue at defined distances from the margin of high-grade PIN or PCa to explore the spatial extension of the sub-visual morphological changes. The described changes appeared to be detectable in the histologically normal-appearing tissue for distances of up to 6 mm from the margin of PIN or PCa [3]. Recently, also, Mairinger et al. [19] reported the presence of changes in the distribution and organization of the nuclear chromatin in cells of non-tumor tissue in vicinity to PCa and compared them with those of BPH nuclei.

There are similarities and differences between the two studies mentioned in the previous paragraph. The great-





est similarity is that both dealt with the evaluation of the chromatin pattern; the results obtained in the two studies were very similar. The differences are that the authors of the first study used hematoxylin and eosin-stained histological sections and that only secretory cells were evaluated [3], whereas the researchers of the other study performed the analysis in Feulgen-stained cell nuclei extracted from the disintegration of 50- $\mu$ m thick sections cut from paraffin blocks [19]. The advantage of the approach of the first group was that the secretory cells were measured at defined distances from a lesion. This could have not been achieved with the approach of the other group due to the type of cytological preparation utilized. This could explain why they used the transition zone tissue for comparison.

An approach similar to that previously adopted by Bartels et al. [3] was followed in our study. This allowed us to use whole-mount sections to obtain accurate information on how diffuse the nuclear changes are and on their exact location within a prostate in relation to areas of PIN and PCa. To the best of our knowledge, ours represents the first detailed attempt to accomplish a complete mapping of the nuclear abnormalities in RP specimens. In this study, it was decided to restrict the analysis to the evaluation of the area, diameter, and form of the nuclei and area of the nucleoli, because these features correspond to those usually routinely evaluated by pathologists, e.g., features related to the size and shape of nuclei and nucleoli.

Recent studies have pointed out that the normal-looking prostate epithelium may also show some molecular changes, such as those concerning glutathione S-transferase and telomerase activity, which are similar to those usually present in the associated preneoplastic and neoplastic lesions [24].

The data in the literature point toward the possibility that in the prostate and other organs, the cases with malignancy-associated cellular markers represent two distinct groups [4, 6, 8, 11, 13, 18, 22, 24, 27]. One could be related to the field effect of the agents that caused the initial lesion, and the other could represent the response to factors secreted by a premalignant or malignant lesion.

Support for the existence of the first group comes from the observation that some abnormalities usually seen in the preneoplastic and neoplastic lesions are occasionally detected in normal-appearing prostate tissue [5, 24]. The changes related to the field effect of the agents that caused the initial lesion might be seen as the onset of the development of prostatic neoplasia [24, 32]. It might well be that under certain conditions, the lesion can progress to a premalignant stage and may then, due to severe genetic instability, result in a clone that has the ability to invade. Data related to the formation of DNA adducts in normal tissue adjacent to cancer in humans support this hypothesis [9, 17]. According to Han et al. [12], the selective occurrence of a DNA adduct in the tissue of origin of carcinomas and preceding carcinoma development suggests a causal relation between adduct for-

mation and prostate cancer development in testosterone plus estradiol-17 beta-treated rats. Further support can be found in studies in which allelic loss was found in normal lobules adjacent to breast cancer [16]. At the morphological level, the genetically altered lobules demonstrated no evidence of hyperplastic or neoplastic changes. According to Dairkee [8], these observations may reflect the existence of a "predisposing field" within which a morphologically normal, yet aberrant, focal area becomes committed to malignant progression, leading eventually to invasive cancer.

Support for the existence of the second group of cases with malignancy-associated cellular markers can be found in a study by MacAulay et al. [18] of bronchial biopsies from patients with and without lung cancer. This investigation showed that changes in the distribution and organization of the nuclear chromatin, defined as malignancy-associated change (MAC), were present in lung cancer patients and absent in healthy individuals. The disappearance of MACs was noted in the subgroup of patients in which the lung with the tumor had been resected. These experimental results support the hypothesis that the changes are due to some communication from already transformed cells to the normal cells in the vicinity. These changes are probably not specific in their nature and might also be seen in association with other lesions, such as inflammation.

It is possible to use the sub-visual morphological changes as a tool in the management of patients with PIN or PCa. In particular, the possibility of identifying cases with subtle alterations may be applicable to specific clinical situations, such as the detection of malignancy in the prostate when only benign-appearing tissue is observed in a biopsy due to inadequate sampling [23].

In conclusion, the normal-looking columnar epithelium from prostates harboring preneoplastic and neoplastic lesions present with diffuse nuclear abnormalities that are not seen by the human eyes but that can be detected with an image analysis system. The changes are hypothesized to represent either the surrounding tissue's response to signals given off by the premalignant or malignant lesion or a response in the surrounding tissue to the field effect of the agents that caused the initial lesion. However, it is not to be excluded that other lesions, such as inflammation, might induce nuclear changes, similar to those we documented here, in normal-looking tissue.

**Notes added in proof** Excerpt from a publication based on the world health organization (WHO) Collaborative Project and Consensus Conference, Stockholm, 8–9 June 2000: "There are four other possible findings in the prostate (low-grade PIN, atypical adenomatous hyperplasia (AAH), malignancy-associated foci, and atrophy) that may be premalignant, but the data for these are much less convincing than that for high-grade PIN" [7].

**Acknowledgements** This research has been supported, in part, by a grant from the University of Ancona. The content of this paper is solely the responsibility of the authors and does not necessarily represent the official views of the University of Ancona. Dr P. Colanzi is a recipient of a fellowship from "Fondazione Italiana per la Ricerca sul Cancro". Dr A. Longatto Filho was a visiting researcher at the University of Ancona.

## References

- Algaba F, Trias I, Lopez L, Rodriguez-Vallejo JM, Gonzales-Esteban J (1995) Neuroendocrine cells in peripheral prostatic zone: age, prostatic intraepithelial neoplasia and latent cancer-related changes. *Eur Urol* 27:329–333
- Bartels PH, da Silva Vinicius D, Montironi R, Hamilton PW, Thompson D, Vaught L, Bartels HG (1998) Chromatin texture signatures in nuclei from prostate lesions. *Anal Quant Cytol Histol* 20:407–416
- Bartels PH, Montironi R, Hamilton PW, Thompson D, Vaught L, Bartels HG (1998) Nuclear chromatin texture in prostate. PIN and malignancy associated changes. *Anal Quant Cytol Histol* 20:397–406
- Bartels PH, Montironi R, Thompson D, Vaught L, Hamilton PW (1998) Statistical histometry of the basal cell/secretory cell bilayer in prostatic intraepithelial neoplasia. *Anal Quant Cytol Histol* 20:381–388
- Berner A, Danielsen HE, Nesland J, Reith A (1996) Prognostic importance of DNA “single” cell aneuploidy in normal, hyperplastic, intraepithelial/carcinomatous prostate (abstract). *Anal Quant Cytol Histol* 18:50
- Bibbo M, Michelassi F, Bartels PH, Dytch H, Bania C, Lerma E, Montag AG (1990) Karyometric marker features in normal-appearing glands adjacent to human colonic adenocarcinoma. *Cancer Res* 50:147–151
- Bostwick D, Montironi R, Sesterhenn IA (2000) Diagnosis of prostatic intraepithelial neoplasia. *Scand J Urol Nephrol* (in press)
- Dairkee SH (1998) Allelic loss in normal lobules adjacent to breast cancer. *Cancer Detection Prevention* 22[suppl 1]:135
- De Waziers I (1998) DNA adduct in normal tissue adjacent to colon cancer. *Cancer Detect Prev* 22[suppl 1]:134
- Epstein JI, Cho KR, Quinn BD (1990) Relationship of severe dysplasia to stage A (incidental) adenocarcinoma of the prostate. *Cancer* 65:2321–2327
- Fleischhacker M, Lee S, Spira S, Takeuchi S, Koeffler P (1995) DNA aneuploidy in morphologically normal colons from patients with colon cancer. *Mod Pathol* 8:360–365
- Han X, Liehr JG, Bosland MC (1995) Induction of a DNA adduct detectable by <sup>32</sup>P-postlabelling in the dorsolateral prostate of NBL/Cr rats treated with estradiol-17 beta and testosterone. *Carcinogenesis* 16:951–954
- Hutchinson ML, Isenstein LM, Martin JJ, Zahniser DJ (1992) Measurement of subvisual changes in cervical squamous metaplastic cells for detecting abnormality. *Analyt Quant Cytol Histol* 14:330–334
- Kovi J, Jackson MA, Heshmat MY (1985) Ductal spread in prostatic carcinoma. *Cancer* 56:1566–1573
- Kovi J, Mostofi FK, Heshmat MY, Enterline JP (1988) Large acinar atypical hyperplasia and carcinoma of the prostate. *Cancer* 61:555–561
- Lakhani SR, Chaggar R, Davies S, Jones C, Collins N, Odel C, Stratton MR, O'Hare MJ (1999) Genetic alterations in “normal” luminal and myoepithelial cells of the breast. *J Pathol* 189:496–503
- Li D, Zhang W, Sahin AA, Hittelman WN (1998) DNA adducts in normal tissue adjacent to breast cancer (abstract). *Cancer Detection Prevention* 22[suppl 1]:134
- MacAulay C, Payne P, Wilton D, Lam S, Palcic B, MAC (1996) Some answers, more questions (abstract). *Analyt Quant Cytol Histol* 19:78
- Mairinger T, Mikuz G, Gschwendtner A (1999) Nuclear chromatin texture analysis of nonmalignant tissue can detect adjacent prostatic adenocarcinoma. *Prostate* 41:12–19
- McNeal JE, Villers A, Redwine EA, Freiha FS, Stamey TA (1991) Microcarcinoma in the prostate: its association with duct-acinar dysplasia. *Hum Pathol* 22:644–652
- McNeal JE, Haillot O, Yemoto C (1995) Cell proliferation in dysplasia of the prostate: analysis by PCNA immunostaining. *Prostate* 27:258–268
- Montag AG, Bartels PH, Lerma-Puertas E, Dytch HE, Leelakusolvong S, Bibbo M (1989) Karyometric marker features in tissue adjacent to in situ cervical carcinomas. *Analyt Quant Cytol Histol* 11:275–280
- Montironi R, Diamanti R, Pomante R, Thompson D, Bartels PH (1997) Subtle changes in benign tissue adjacent to prostate neoplasia detected with a bayesian belief network. *J Pathol* 182:442–449
- Montironi R, Hamilton PW, Scarpelli M, Thompson D, Bartels PH (1999) Subtle morphological and molecular changes in normal-looking epithelium in prostates with prostatic intraepithelial neoplasia or cancer. *Eur Urol* 35:468–473
- Montironi R, Thompson D, Bartels PH (1999) Premalignant lesions of the prostate. In: Lowe DG, Underwood JCE (eds) *Recent advances in histopathology* no. 18. Churchill Livingstone, London, pp 147–172
- Montironi R, Mazzucchelli R, Algaba F, Lopez Beltran A (2000) Morphological identification of the pattern of prostatic intraepithelial neoplasia and their significance. *J Clin Path* 53:655–665
- Nieburgs H (1992) Malignancy-associated cellular markers. In: Wied GL, Keebler CM, Koss LG, Patten SF, Rosenthal DL (eds) *Compendium on diagnostic cytology* 7th edn. *Tutorials of cytology*, Chicago, pp 409–418
- Qian J, Bostwick DG (1995) The extent and zonal location of prostatic intraepithelial neoplasia and atypical adenomatous hyperplasia: relationship with carcinoma in radical prostatectomy specimens. *Pathol Res Pract* 191:860–867
- Qian J, Jenkins RB, Bostwick DG (1997) Detection of chromosomal anomalies and c-myc gene amplification in the cribriform pattern of prostatic intraepithelial neoplasia and carcinoma by fluorescence in situ hybridization. *Mod Pathol* 10:1113–1119
- Quinn BD, Cho KR, Epstein JI (1990) Relationship of severe dysplasia to stage B adenocarcinoma of the prostate. *Cancer* 65:2328–2337
- Sakr WA, Grignon DJ, Haas GP, Heilbrun LK, Pontes JE, Crissman JD (1996) Age and racial distribution of prostatic intraepithelial neoplasia. *Eur Urol* 30:138–144
- Sandberg AA (1998) Chromosomal abnormalities in human prostate cancer: their detection and pathological significance. In: Foster CS, Bostwick DG (eds) *Pathology of the prostate. Major problems in pathology*. Saunders, Philadelphia, pp 400–427